Extreme Mechanics Letters 49 (2021) 101463

Contents lists available at ScienceDirect

Extreme Mechanics Letters

journal homepage: www.elsevier.com/locate/eml

Peristalsis-like migration of carbon-metabolizing catalytic nanoparticles

Peng-Han Lu [a,1], De-Gang Xie [a], Bo-Yu Liu [a], Fei Ai [a], Zhao-Rui Zhang [b], Ming-Shang Jin [b], Xiao Feng Zhang [c], En Ma [d], Ju Li [e,*], Zhi-Wei Shan [a]

[a] Center for Advancing Materials Performance from the Nanoscale, State Key Laboratory for Mechanical Behavior of Materials, Xi'an Jiaotong University, Xi'an 710049, China
[b] Frontier Institute of Science and Technology and State Key Laboratory of Multiphase Flow in Power Engineering, Xi'an Jiaotong University, Xi'an 710049, China
[c] Nanosys Inc., Milpitas, CA 95035, USA
[d] Center for Alloy Innovation and Design, State Key Laboratory for Mechanical Behavior of Materials, Xi'an Jiaotong University, Xi'an 710049, China
[e] Department of Nuclear Science and Engineering and Department of Materials Science and Engineering, Massachusetts Institute of Technology, Cambridge, MA 02139, USA

ARTICLE INFO

Article history:
Received 18 July 2021
Accepted 11 August 2021
Available online 17 September 2021

Keywords:
Peristaltic locomotion
Surface diffusion
Heterogeneous catalysis
Carbon removal
Metallic nanoparticles
Environmental transmission electron microscopy

ABSTRACT

Translational and rotational motion of solid matter is normally driven by external physical forces. Here we report that under oxygen atmosphere inside an environmental transmission electron microscope, catalytic palladium nanoparticles underwent a self-propelled, peristalsis-like locomotion on a supporting substrate at a relatively low temperature. Surprisingly, the particles maintained crystalline interior and even conserved their initial crystal orientations during the dramatic liquid-like motion. Such "peristaltic" crystal migration with shape oscillation is found to be mediated by profuse surface diffusion, under chemical driving forces from palladium-catalyzed gaseous oxidation of a carbonaceous layer. These findings open a new avenue of efficient heterogeneous catalysis, and reveal emergent behavior that can arise out of an energy-metabolizing nano-system.

Supported metal nanoparticles form the basis of many heterogeneous catalytic reactions of industrial importance [1]. Although the past decade has witnessed an explosion of elegantly synthesized metal nanocrystals with controlled compositions, sizes, shapes and structures [2,3], these characteristics may evolve under reactive conditions. The nanocatalysts often experience dynamic evolution in response to the surrounding gaseous environment, including sintering/redispersion [4,5], shape transition [6,7], surface reconstruction [8–10], surface segregation [11–13], phase transformation [14,15], etc. These dynamic changes usually correlate with their catalytic reactivity. For example, the morphology change of metal nanocrystals was found to bring about a transient [16] or oscillatory [17] reaction kinetics. Therefore, many efforts have been undertaken to stabilize or anchor the nanoparticles with a fixed shape and position during catalysis [18,19]. However, inspired by enzyme catalysts in biology which usually exhibit shape flexibility and spatial mobility, and recent findings that metal nanostructures can experience fast transformation dynamics through surface diffusion [20,21], one may alternatively take advantage of these dynamic changes to realize a "living" catalytic process even in non-biological systems.

Here, we demonstrate a lifelike catalysis with palladium nanoparticles (Pd NPs) catalyzing the oxidation of carbon. Pd NPs of diameter ~10 nm were dispersed in ethanol under sonication and then dropped onto a ~50 nm-thick, amorphous SiN_x membrane. Using a differentially pumped gas-environmental transmission electron microscope (Hitachi H-9500 ETEM) and a microchip-based heating stage, a direct visualization of the particle dynamics under oxygen atmosphere and at elevated temperature were obtained. The schematic illustration of the experimental setup is shown in Supplementary Fig. S1.

The particles were firstly heated up to ~300 °C in vacuum. They stayed immobile even after half an hour except that the shape of some particles became a little round. Surprisingly, after a pure oxygen atmosphere was established around the sample with a partial pressure of ~0.2 Pa, some particles became "nanomotors" roaming around, but would become stationary again if the oxygen flow was cut off (see more details in Supplementary

* Corresponding author.
E-mail addresses: maen@xjtu.edu.cn (E. Ma), liju@mit.edu (J. Li), zwshan@xjtu.edu.cn (Z.-W. Shan).

[1] Present address: Ernst Ruska-Centre for Microscopy and Spectroscopy with Electrons and Peter Grünberg Institute, Forschungszentrum Jülich, 52425 Jülich, Germany.

https://doi.org/10.1016/j.eml.2021.101463
2352-4316/

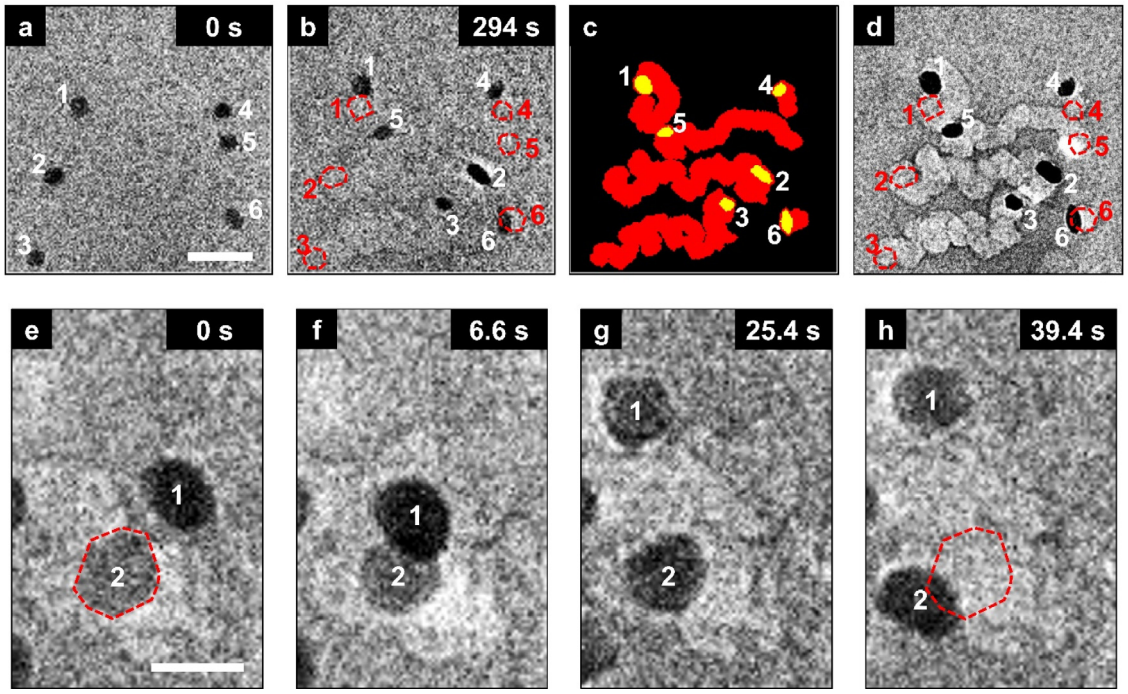

Fig. 1. Self-propelled migration and contagious mobilization of Pd NPs. a–d, Self-propelled locomotion of Pd NPs under 0.2 Pa pure oxygen at 300 °C. The moving trajectories (**c**) of particles between the initial (**a**, red circles in **b** and **d**) and final (**b**) state coincide with the channels on the substrate found in the final state at under-focus imaging mode (**d**). Scale bar, 50 nm. **e–h**, Time-lapsed TEM images of Pd NPs at the same reaction condition, showing a "contagious mobilization" behavior. After the contact with the mobile Particle 1, Particle 2 (delineated by dashed red polygon in **e** and **h**) started migrating away from its initial position (**g, h**). Scale bar, 20 nm. See Supplementary Movie S1 and S2.

Materials Table S1). One typical example is illustrated in Fig. 1a–d. Fig. 1a, b displays the beginning (oxygen injection) and final (oxygen cut off) state of the particles, respectively. It can be seen that all of the six particles moved away from their initial positions. From the *in situ* movie data (Supplementary Movie S1), the moving trajectory of each of them was mapped out in Fig. 1c. These particles, however, did not show a universal moving direction, but seemed to move around semi-randomly like in Brownian motion. A check of the final state in the under-focus imaging mode demonstrated several etched channels on the substrate. Interestingly, those channels (Fig. 1d) coincided exactly with the trajectories of the particles extracted from the recorded movie (Fig. 1c), while in other areas where particles never passed by, no such channels could be found. The channels were seen to be self-avoiding. That is, a particle would not cross the previous track of any other particles. Therefore, the random walks of these particles are not history-independent but has interesting non-Markovian (history-dependent) and multi-particle correlated features. More startlingly, when a moving particle (Particle 1 in Fig. 1e–h) happened to touch a stationary one (Particle 2 in Fig. 1 e–h), the initially-dormant particle would start migrating with its shape simultaneously changing after contact (Supplementary Movie S2). We termed this phenomenon "contagious mobilization".

The lifelike dynamics of the nanoscale particle ensemble cannot be rationalized by equilibrium thermodynamics, but is, in all likelihood, driven by active chemical energy dissipation (metabolism). In order to unveil the mechanism of aforementioned phenomena, local chemical characterization using high angle annular dark field-scanning TEM (HAADF-STEM) imaging and electron energy loss spectroscopy (EELS) was performed around the channels. Fig. 2b presents a series of core-loss spectra collected across a channel shown in Fig. 2a. The nitrogen (N) K peak deriving from the SiN_x membrane existed in all the spectra, while the carbon (C) K peak could only be detected in spectra 1&4 (outside the channel). This demonstrated that a carbonaceous layer has been consumed during the migration process of the particle. Detailed analysis suggested that the carbonaceous layer resulted from the residue surfactant polymers (see more details in Supplementary Materials and Fig. S2). On the other hand, the nanobeam diffraction pattern of Pd NPs demonstrated that they remained face-centered cubic palladium structure after the reaction, instead of forming carbides or oxides (Supplementary Fig. S3). Therefore, it can be inferred that the carbonaceous layer over the SiN_x substrate was oxidized into volatile carbon monoxide (CO) or carbon dioxide (CO_2) through the palladium-catalyzed reaction with oxygen at relatively low temperatures, and hence the carbon-deficient etched channels were created accompanying the migration of Pd NPs.

Since the catalytic carbon oxidation is initiated by the chemisorption of oxygen on the Pd surface, a dense surface carbonaceous layer over the NPs would serve as a kinetic barrier to prevent the oxygen from directly contacting the catalyst, and thus prohibit the catalytic reaction. This is the basic mechanism behind catalyst deactivation by coking in chemical industries [22]. However, these barricades are not all uniform and may evolve with the temperature rise. Some particles with bald spots on the surface barrier layer could adsorb the oxygen, facilitate the metabolism of carbon over the particle surface (see the *in situ* high resolution ETEM results in Supplementary Fig. S4) as well as around the particle, and thus become the "pioneers" moving around (e.g. Fig. 1a–d). Moreover, a mobile NP will also, upon contact, help to remove the protective carbon shell of an initially-dormant particle it touches, as illustrated in Fig. 2 c–f. As a result of this "contagious mobilization" via decoking of the surfaces, more particles will be activated upon encountering mobile particles, which will then start to move themselves. This is thus a self-propelling chain reaction of mobilization and decoking.

By analyzing the morphological dynamics of the particles during the whole process, we found an oscillatory elongation–contraction shape transition behavior and a concomitant "peristaltic" locomotion. Fig. 3 a–d, are four typical snapshots from

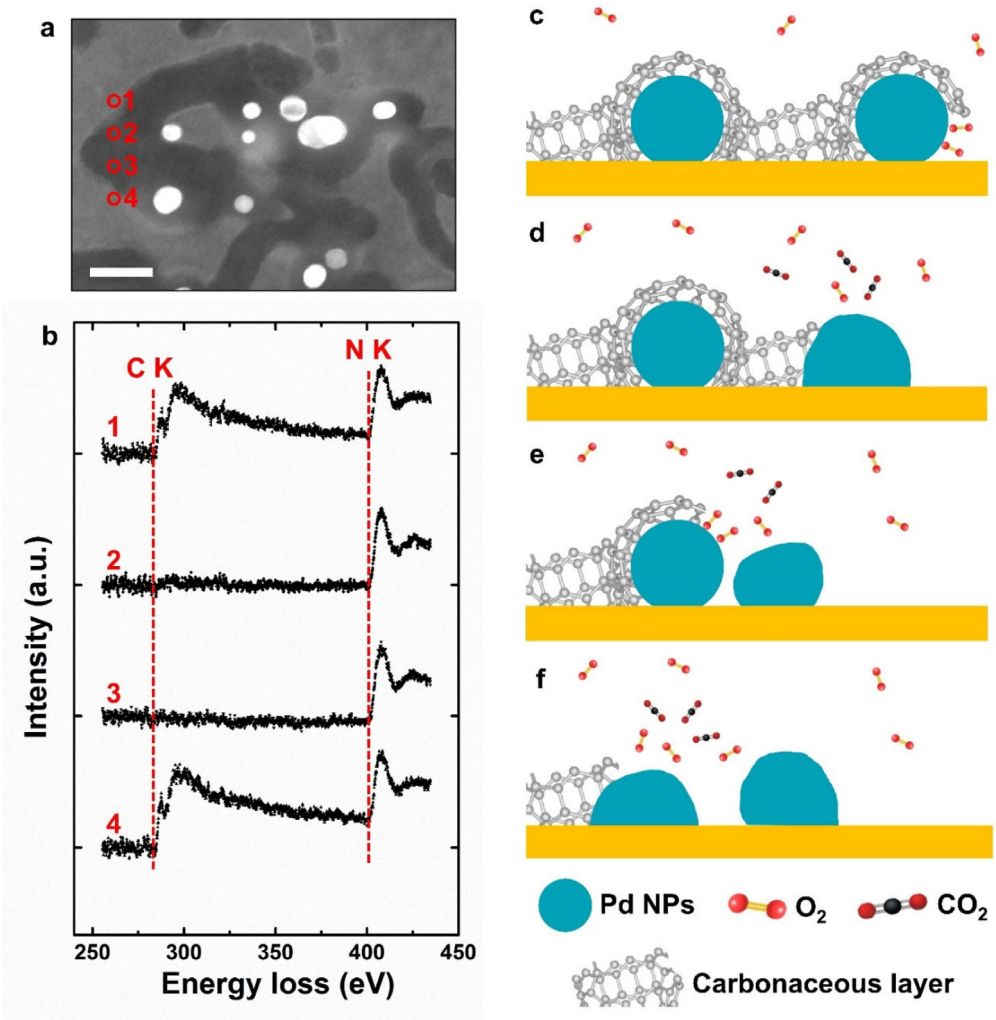

Fig. 2. Carbon-metabolizing mechanism. a, HAADF-STEM image of the carved channels by particles migration. Scale bar, 50 nm. **b**, The corresponding electron energy loss spectra collected at the positions marked in (**a**) demonstrated that carbon was consumed inside the channel. **c–f**, Schematic illustration of the chain-reaction resulted from self-activation and contiguous activation.

an *in situ* movie (Supplementary Movie S3) demonstrating the contraction (Fig. 3a and c) and elongation (Fig. 3b and d) in particle shape. In order to quantitatively describe the extent of deformation, the circumscribed ellipse of the particle was used to mimic its profile. The evolution of the eccentricity of the ellipse is plotted in Fig. 3e. It shows that the eccentricity quasi-periodically fluctuates between 0.65 (relatively round) and 0.93 (much more elongated), indicating a morphological oscillation of the particle. This thereupon gave rise to a peristalsis-fashion migration of the particle, which is akin to the movement of the earthworm by the means of alternately shortening and lengthening its body.

Furthermore, when observed out of focus, some shadow images with bright contrast (red crosses in Fig. 4a–f) were displaced from the particle (red spots in Fig. 4 a–f), and appeared intermittently at some certain angles (Fig. 4g) during the particle migration (Supplementary Movie S6). The formation of these shadow images resulted from the image delocalization of the corresponding particle at large defocus setting. The shifts of the delocalization relative to the particle should move in the direction of the vectors of the strongly excited diffraction beams, and the distances in between should be inversely proportional to the interspacing of the corresponding crystal plane [23]. Therefore it is particularly striking to find that the polar coordinates of the relative distance and azimuth angle (red crosses in Fig. 4h) coincided well with the diffraction pattern of a face-centered cubic structure under [100] zone axis (blue dots in Fig. 4h). It presents a persuasive evidence to prove that the active particle, although behaving like liquids morphologically, always had a crystalline interior, and was always traveling under, or at least close to, one fixed zone axis during its migration. This suggests that the locomotion did not involve obvious rigid-body rotation, but was dominated by surface diffusion.

Physically, the particle movements are accomplished by Coble creep, that is, surface diffusion of Pd atoms, which happens so rapidly at this length scale that it is sufficient to sustain the mass transport needed for the shape changes [20]. The key difference with traditional Coble creep is that it is driven by chemical energy release instead of mechanical energy release or capillary energy reduction [20]; that is, the Pd atoms diffuse to where $C+O^{*}\rightarrow CO\uparrow$ or $CO_2\uparrow$ can happen. Consequently, the Pd particle is then motivated to spread part of itself towards the neighboring carbon, protruding in a way that allows it to catch carbon to engage in further catalytic reaction. This results in the observed "elongation", as the ends appear as if they were anchored and "stretched" by the carbon borderline that is receding away from the particle. However, the catalytic etching perpendicular to the carbon borderline might experience different speeds at each point, especially at both ends of the particle due to the perturbation of the surface diffusion of Pd atoms parallel to the borderline. As a result, the slope of the carbon borderline and thus the elongation

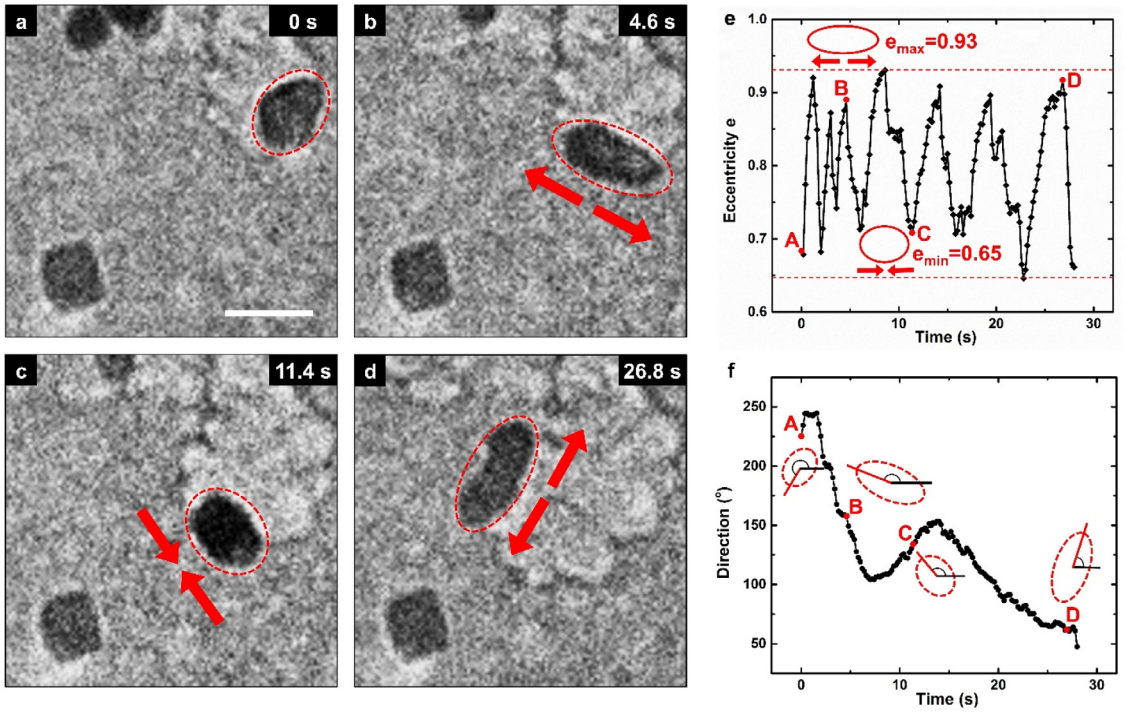

Fig. 3. Peristalsis-like locomotion of a Pd NP. a–d, *In situ* TEM snapshots illustrating an elongation–contraction oscillatory evolution of a Pd NP during its migration. Scale bar, 20 nm. See Supplementary Movie S3. **e**, Time-dependent evolution of the eccentricity of the particle geometry as delineated by the circumscribed ellipses in **a–d**. **f**, Time-dependent elongation direction of the particle. The direction is denoted by the angle between the horizontal line and one fixed end of the long axis of the ellipse. The four insets correspond to **a–d**.

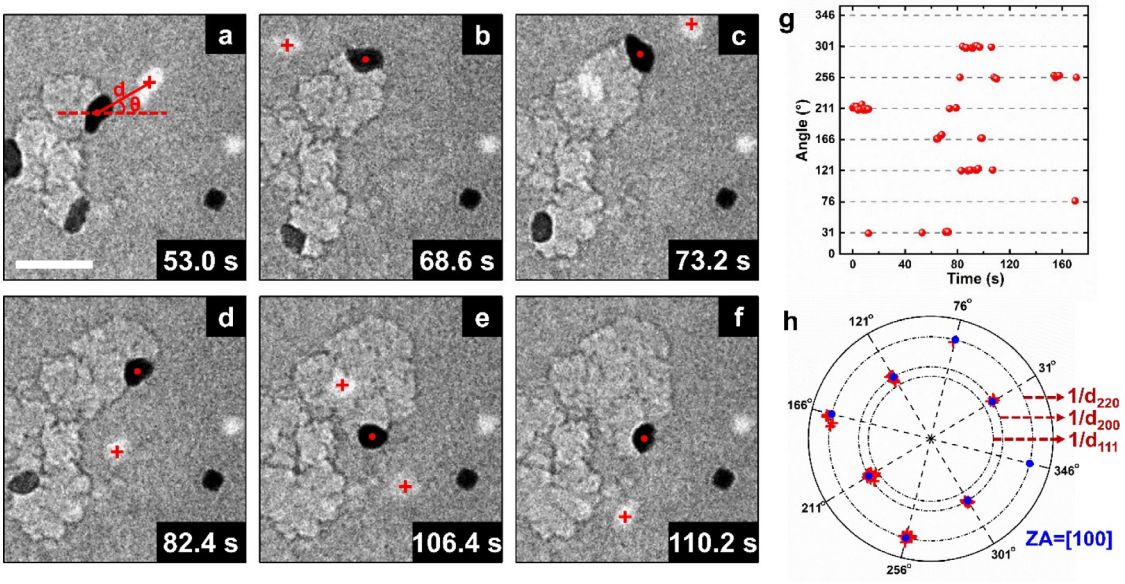

Fig. 4. Orientation-conserved crystal migration. a–f, Snapshots from an *in situ* movie in the under-focus imaging mode. The shadow images with bright contrast could be found near the particles. Scale bar, 50 nm. **g**, Time-dependent positions of the shadow image marked with red "+" symbol in **a–f**. **h**, Polar coordination diagram showing, as red crosses, the azimuth angle and relative distance between the shadow image and the particle. The blue dots illustrate a diffraction pattern of a face-centered cubic structure under [100] zone axis. See Supplementary Movie S6.. (For interpretation of the references to color in this figure legend, the reader is referred to the web version of this article.)

direction of the particle were modified constantly, as indicated by the angles between the horizontal line and one fixed end of the long axis of the ellipse which are plotted in Fig. 3f. On the other hand, the particles do not elongate indefinitely, and would sometime shrink towards a more spherical shape driven by surface energy minimization. This competition between active catalytic metabolism of the surroundings and self-energy minimization provokes the shape oscillation and "peristaltic" migration of Pd NPs.

The liquid-like, orientation-conserved crystal migration through profuse diffusion can be best displayed in a bi-grained particle in Fig. S5. As shown in Fig. S5a, a particle, possibly fused by smaller ones, included two grains with a grain boundary (GB) along the red dashed line, which was inferred from the

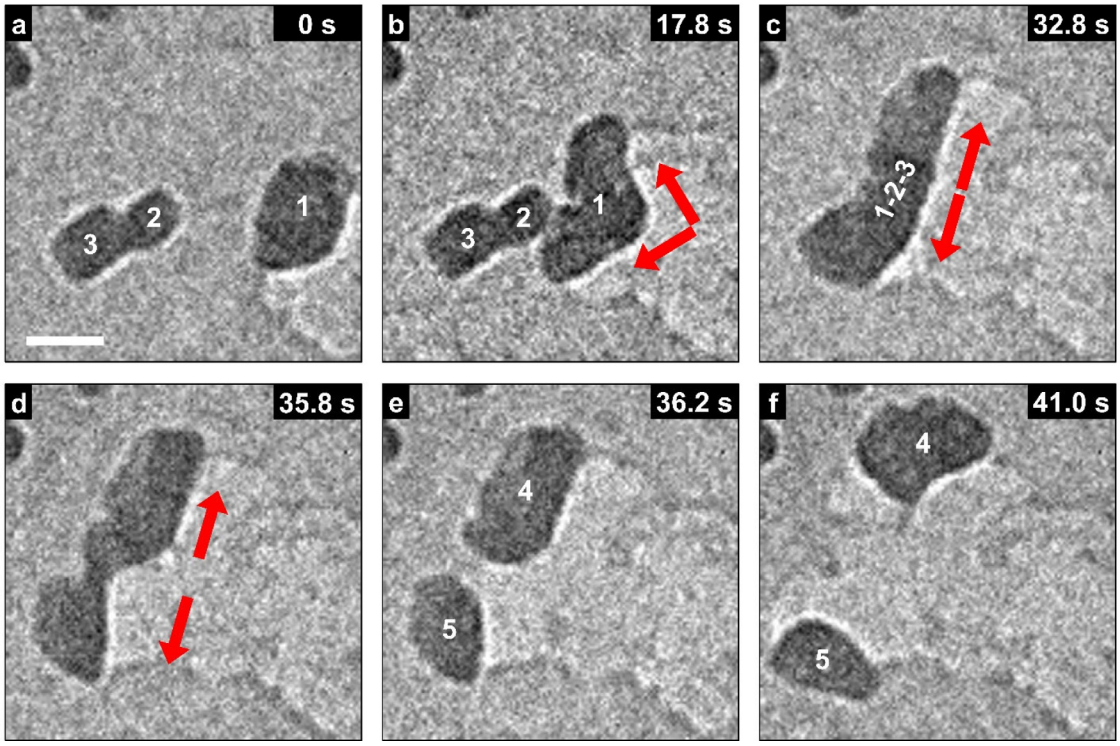

Fig. 5. Fusion and fission of nanoparticles. a–c, Fusion of the particles. Particle 1 moved around and coalesced with Particles 2&3 into a larger one. **d–f**, Fission of a larger particle and the split particles were then able to move around as independent entities. Scale bar, 20 nm. See Supplementary Movie S4.

distinct diffraction contrast of the two halves (one darker, one brighter). Instead of undergoing grain rotation or grain boundary migration that are often found at high temperature [24,25], or under mechanical stress [26,27], the particle retained its grain boundary along the red dashed line with constant slope and abscissa, swinging around it and catalyzing the oxidation of the carbon on both sides (Supplementary Movie S5). This process was realized through surface self-diffusion of the Pd atoms, that is, the mass on one side traveled through the surface of the particle to the other side, so the grain boundary must remain pinned to that line in both slope and abscissa. The projected area of both sides underwent an oscillatory change alternately (Fig. S5e). When and only when the mass of either side was completely transported to the other one, the particle would be depinned from that GB line (since GB has disappeared) and be able to freely move in two dimensions again as a single-grained NP (Fig. S5d).

Albeit the flexible shape and complex interactions, the Pd NPs could sometimes preserve their individual identity much longer than one expects. In Fig. 1e–h, for example, the two particles separated again even after contact, as in most of the contagious mobilization encounters. This is opposite to capillary energy minimization mechanism which always favors particle coalescence, and imparts the impression of living organisms. In addition, we found that particle coalescence can be counteracted statistically by particle splitting, analogous to the cell fusion and fission in biology. One typical example is shown in Fig. 5 (Supplementary Movie S4). Three particles coalesced and then underwent shape elongation. However, soon after, this coalesced particle split into two, like in biological cell division. This splitting is an alternative process to the particle contraction: there seems to be a critical neck thickness below which the polarizing influence of the carbon on the two ends is too great to maintain unity. The split particles were then able to move around as independent entities.

As either the density of the NPs increases, or the carbon resources nearby get exhausted, the NPs will migrate less, split off less and eventually turn into immobile particles that slowly coarsen, and the system will demonstrate less "living" but more near-equilibrium features. We conjecture based on our understanding of the dynamics, however, that if one were able to replenish carbon on the substrate continuously as in many actual industrial processes, then fusion and fission events of NPs might balance statistically, and we should achieve a NP population at quasi-steady state, because the principle of maximum entropy production rate in non-equilibrium thermodynamics calls for many small NPs with long total carbon-Pd contact lines to metabolize carbon, rather than a gigantic fused particle favored by equilibrium thermodynamics.

In conclusion, we have discovered a motile decoking nanocatalytic system that works via peristalsis-like migration and contagious mobilization, with crystalline interior and strongly conserved crystallographic orientation. This lifelike dynamics of inorganic matter represents a startling emergent behavior that can arise out of an energy-metabolizing nano-system, and may inspire more flexible and efficient use of nanostructures in engineering applications such as anti-coking catalysts, self-cleaning surfaces, soft robotic systems and biomimetic machines.

CRediT authorship contribution statement

Peng-Han Lu: performed the *in situ* ETEM experiments, conducted the STEM-EELS characterization, analyzed the data, and wrote the manuscript. **De-Gang Xie:** analyzed the data, discussed the results and commented on the manuscript. **Bo-Yu Liu:** conducted the STEM-EELS characterization, discussed the results and commented on the manuscript. **Fei Ai:** analyzed the data, discussed the results and commented on the manuscript. **Zhao-Rui Zhang:** synthesized the nanoparticle sample, discussed the results and commented on the manuscript. **Ming-Shang Jin:** synthesized the nanoparticle sample, discussed the results and commented on the manuscript. **Xiao Feng Zhang:** discussed the results and commneted on the manuscript. **En Ma:** supervised the project, discussed

the results and revised the manuscript. **Ju Li:** supervised the project, discussed the results and wrote the manuscript. **Zhi-Wei Shan:** supervised the project, discussed the results and revised the manuscript.

Declaration of competing interest

The authors declare that they have no known competing financial interests or personal relationships that could have appeared to influence the work reported in this paper.

Acknowledgments

Z.-W.S. acknowledges supports from National Natural Science Foundation of China (52031011), the National Key Research and Development Program of China (No. 2017YFB0702001). E.M. acknowledges XJTU, China for supporting his work at CAID. The authors acknowledge the support by the International Joint Laboratory for Micro/Nano Manufacturing and Measurement Technologies, China of XJTU. We also thank Dr. Chao Wu (Xi'an Jiaotong University, Xi'an, China) and Prof. Kaili Jiang (Tsinghua University, Beijing, China) for helpful discussions. J.L. acknowledges support by NSF CBET-2034902.

Appendix A. Supplementary data

Supplementary material related to this article can be found online at https://doi.org/10.1016/j.eml.2021.101463.

References

[1] G.A. Somorjai, Y. Li, Introduction To Surface Chemistry and Catalysis, John Wiley & Sons, 2010.
[2] Y. Xia, Y. Xiong, B. Lim, S.E. Skrabalak, Shape-controlled synthesis of metal nanocrystals: Simple chemistry meets complex physics? Angew. Chem. Int. Ed. 48 (2009) 60–103.
[3] J. Lu, J.W. Elam, P.C. Stair, Synthesis and stabilization of supported metal catalysts by atomic layer deposition, Acc. Chem. Res. 46 (2013) 1806–1815.
[4] M.A. Newton, C. Belver-Coldeira, A. Martinez-Arias, M. Fernandez-Garcia, Dynamic in situ observation of rapid size and shape change of supported Pd nanoparticles during CO/NO cycling, Nature Mater. 6 (2007) 528–532.
[5] Y. Li, et al., Complex structural dynamics of nanocatalysts revealed in Operando conditions by correlated imaging and spectroscopy probes, Nature Commun. 6 (2015) 7583.
[6] P.L. Hansen, et al., Atom-resolved imaging of dynamic shape changes in supported copper nanocrystals, Science 295 (2002) 2053–2055.
[7] S. Hofmann, et al., In situ observations of catalyst dynamics during surface-bound carbon nanotube nucleation, Nano Lett. 7 (2007) 602–608.
[8] F. Tao, et al., Break-up of stepped platinum catalyst surfaces by high CO coverage, Science 327 (2010) 850–853.
[9] H. Yoshida, et al., Visualizing gas molecules interacting with supported nanoparticulate catalysts at reaction conditions, Science 335 (2012) 317–319.
[10] J. Gustafson, et al., High-energy surface X-ray diffraction for fast surface structure determination, Science 343 (2014) 758–761.
[11] T.W. Hansen, et al., Atomic-resolution in situ transmission electron microscopy of a promoter of a heterogeneous catalyst, Science 294 (2001) 1508–1510.
[12] F. Tao, et al., Reaction-driven restructuring of Rh-Pd and Pt-Pd core–shell nanoparticles, Science 322 (2008) 932–934.
[13] H.L. Xin, et al., Revealing the atomic restructuring of Pt–Co nanoparticles, Nano Lett. 14 (2014) 3203–3207.
[14] E. de Smit, et al., Nanoscale chemical imaging of a working catalyst by scanning transmission X-ray microscopy, Nature 456 (2008) 222–225.
[15] S. Chenna, R. Banerjee, P.A. Crozier, Atomic-scale observation of the Ni activation process for partial oxidation of methane using in situ environmental TEM, Chem. Cat. Chem. 3 (2011) 1051–1059.
[16] P.C. Vesborg, et al., Transient behavior of Cu/ZnO-based methanol synthesis catalysts, J. Catal. 262 (2009) 65–72.
[17] S.B. Vendelbo, et al., Visualization of oscillatory behaviour of Pt nanoparticles catalysing CO oxidation, Nat. Mater. 13 (2014) 884–890.
[18] J.J. Liu, Advanced electron microscopy of metal–support interactions in supported metal catalysts, Chem. Cat. Chem. 3 (2011) 934–948.
[19] S. Schauermann, N. Nilius, S. Shaikhutdinov, H.J. Freund, Nanoparticles for heterogeneous catalysis: new mechanistic insights, Acc. Chem. Res. 46 (2013) 1673–1681.
[20] J. Sun, et al., Liquid-like pseudoelasticity of sub-10-nm crystalline silver particles, Nature Mater. 13 (2014) 1007–1012.
[21] D.G. Xie, et al., In situ study of the initiation of hydrogen bubbles at the aluminium metal/oxide interface, Nat. Mater. 14 (2015) 899–903.
[22] J.A. Moulijn, A. Van Diepen, F. Kapteijn, Catalyst deactivation: is it predictable?: What to do? Appl. Catal. A: General 212 (2001) 3–16.
[23] H. Zandbergen, D. Tang, D. Van Dyck, Non-linear interference in relation to strong delocalisation, Ultramicroscopy 64 (1996) 185–198.
[24] J.M. Yuk, et al., In situ atomic imaging of coalescence of Au nanoparticles on graphene: rotation and grain boundary migration, Chem. Commun. (Camb) 49 (2013) 11479–11481.
[25] M.A. van Huis, et al., Low-temperature nanocrystal unification through rotations and relaxations probed by in situ transmission electron microscopy, Nano Lett. 8 (2008) 3959–3963.
[26] Z.W. Shan, et al., Grain boundary-mediated plasticity in nanocrystalline nickel, Science 305 (2004) 654–657.
[27] T.J. Rupert, D.S. Gianola, Y. Gan, K.J. Hemker, Experimental observations of stress-driven grain boundary migration, Science 326 (2009) 1686–1690.

Supporting Materials for

Peristalsis-like migration of carbon-metabolizing catalytic nanoparticles

Peng-Han Lu[1†], De-Gang Xie[1], Bo-Yu Liu[1], Fei Ai[1], Zhao-Rui Zhang[2], Ming-Shang Jin[2], Xiao Feng Zhang[3], En Ma[4*], Ju Li[5*] and Zhi-Wei Shan[1*]

[1]Center for Advancing Materials Performance from the Nanoscale, State Key Laboratory for Mechanical Behavior of Materials, Xi'an Jiaotong University, Xi'an 710049, China

[2]Frontier Institute of Science and Technology and State Key Laboratory of Multiphase Flow in Power Engineering, Xi'an Jiaotong University, Xi'an 710049, China

[3]Nanosys Inc., Milpitas, CA 95035, USA

[4]Center for Alloy Innovation and Design, State Key Laboratory for Mechanical Behavior of Materials, Xi'an Jiaotong University, Xi'an 710049, China

[5]Department of Nuclear Science and Engineering and Department of Materials Science and Engineering, Massachusetts Institute of Technology, Cambridge, MA 02139, USA

[†]Present address: Ernst Ruska-Centre for Microscopy and Spectroscopy with Electrons and Peter Grünberg Institute, Forschungszentrum Jülich, 52425 Jülich, Germany

*E-mail: maen@xjtu.edu.cn; liju@mit.edu; zwshan@xjtu.edu.cn

Synthesis of Pd nanoparticles. Pd cubic seeds with an average edge length of 10 nm were synthesized following a previously reported protocol[1]. In a typical synthesis experiment, 8.0 mL of deionized (DI) water (18.2 MΩ·cm), 105 mg of Poly(vinyl pyrrolidone) (PVP, MW≈55,000, Aldrich), 60 mg of L-ascorbic acid (AA, Aldrich), and 300 mg of KBr (Aldrich) were mixed together in a 20 mL vial and pre-heated in air under magnetic stirring at 80 ºC for 10 min. 57 mg of Na_2PdCl_4 (Aldrich) were dissolved in 3 mL of DI water and then introduced into the pre-heated solution. After the vial had been capped, the reaction was allowed to proceed at 80 ºC for 3 h. The final product was collected by centrifugation.

***In situ* heating ETEM experiments.** The *in situ* heating experiments were carried out on a micro-electro-mechanical system (MEMS) thermal chip (Protochips Aduro heating holder). Pd NPs were dispersed in ethanol under sonication and dropped onto a MEMS chip for the *in situ* TEM experiments. They were directly heated up to 300 ºC at a heating rate of 2 ºC/s and kept at that temperature for ~30 min. Pure oxygen gas up to 0.2 Pa was then injected into the TEM specimen chamber. The dynamics of Pd NPs under oxygen atmosphere were investigated with Hitachi H-9500 environmental transmission electron microscope (ETEM) operated at 300 keV. The microscope is featured by a differentially pumped system and thus can accommodate reactive gases within the specimen chamber. The real-time TEM movies were recorded with Gatan Orius 832 high-speed charge coupled device (CCD) camera at a time resolution of 0.2 s.

Schematic illustration of the experimental setup

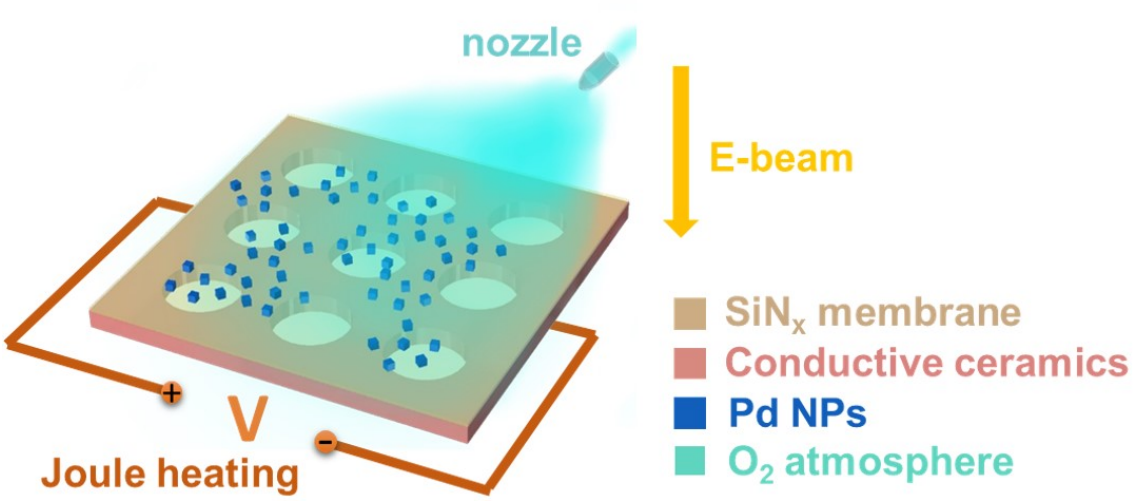

Supplementary Figure S1 | Pd NPs of diameter ~10 nm were dropped onto a ~50 nm-thick, amorphous SiN_x membrane on a MEMS thermal chip for the *in situ* TEM experiments. Pure oxygen gas was then injected into the TEM specimen chamber. Using a differentially pumped gas-environmental transmission electron microscope (Hitachi H-9500 ETEM) and a microchip-based Joule-heating stage, a direct visualization of the particle dynamics under oxygen atmosphere and at elevated temperature were obtained.

HAADF-STEM, NBED and EELS characterization. Further characterization was performed using High Angle Annular Dark Field Scanning TEM (HAADF-STEM) imaging, Nano-Beam Electron Diffraction (NBED) and Electron Energy-Loss Spectroscopy (EELS) after the *in situ* reaction inside ETEM. The samples on the microchip were reloaded to another TEM (JEOL JEM-2100F) with compatible holder for this characterization.

Critical conditions for the self-propelled motion of Pd particles

Supplementary Table S1

	RT	100 °C	200 °C	300 °C
Vacuum (2e-4 Pa)	**F**	**F**	**F**	**F**
O_2 (2e-1 Pa)	**F**	**F**	**F**	either w/ or w/o e-beam **T**
N_2 (2e-1 Pa)	**F**	**F**	**F**	**F**

F: No obvious motion T: Rapid dramatic motions

From Table S1, it can be determined that the oxygen atmosphere and an elevated temperature (much lower than the melting point of Pd but still a little higher than room temperature) are necessary for this reaction, while e-beam irradiation is not required.

Source of the carbonaceous layer

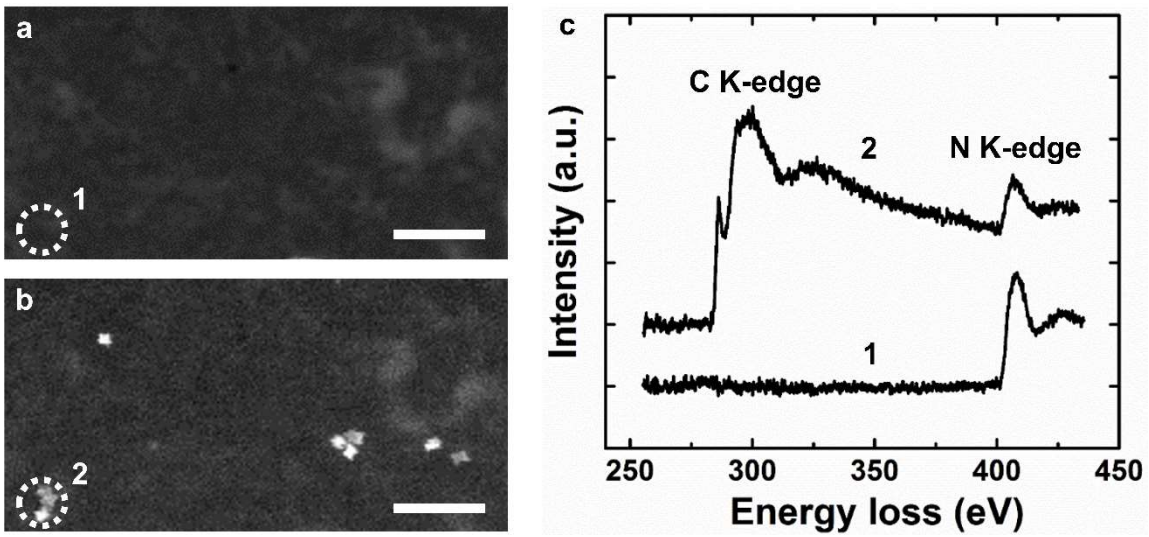

Supplementary Figure S2 | HAADF-STEM images of (**a**) a fresh SiN_x support without any samples and (**b**) the same position after dispersing Pd NP samples. Electron energy loss spectra (**c**) showed that notable carbon signal could only be detected after depositing the samples on the substrate. All scale bar, 100 nm.

We examined several possible origins of the source of the carbonaceous layer. First, electron beam irradiation-induced carbon contamination can be ruled out, because in the beam-off condition the particles still experienced similar dynamic evolution (Table S1). Second, EELS characterization of a fresh SiN_x support without any samples exhibited little carbon signal. However, after dropping Pd NP samples, notable carbon signal could be detected at the same position (Fig. S2). Therefore, the carbon source should come from the sample solution. Third, it has been reported that most of the surfactant polymers, which are often used in the shape-controlled synthesis of nanomaterials, could hardly be washed away completely through centrifugation[2], especially when the size of the NPs decreases down to ~10 nm. The residue surfactant polymers after air drying and vacuum annealing will transform into a carbonaceous layer. This was further confirmed by *in situ* high resolution TEM (HRTEM) study of an individual Pd NP. As presented in Supplementary Fig. S4, it was obvious that there was an amorphous layer over the surface of the particle, which should come from the surface coating surfactants. Similar to what we found about the carbonaceous layer over the substrate, the amorphous layer on NP surface could also be removed under oxygen atmosphere.

Structure of the Pd NP after the reaction

Nano-beam diffraction characterization of the Pd NP after the reaction showed that the particles remained face-centered cubic structure, instead of forming carbide or oxide. One typical example is given in Fig. S3.

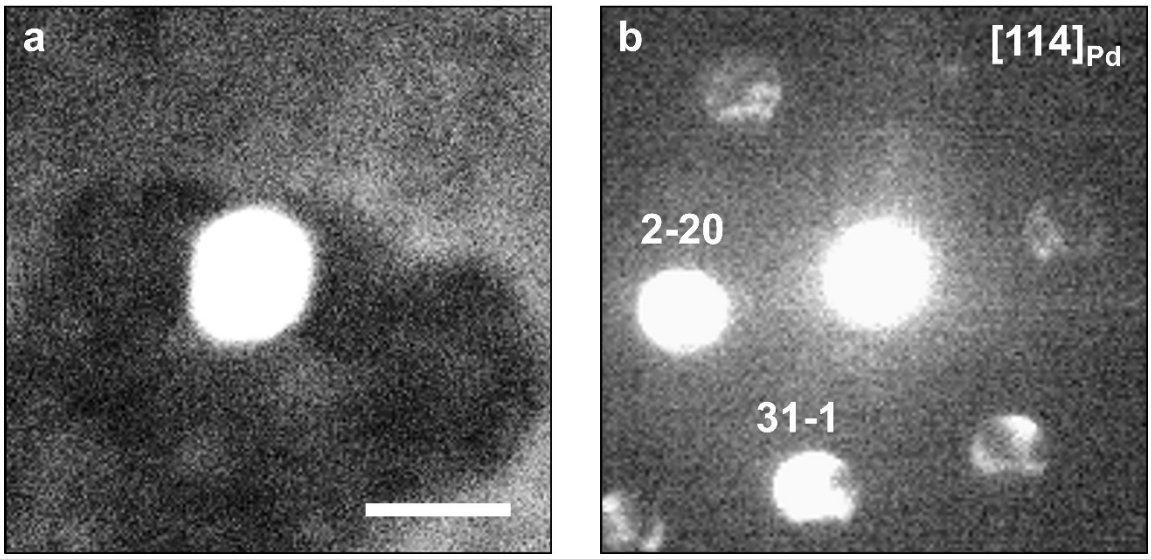

Supplementary Figure S3 | HAADF-STEM image (**a**) and nano-beam diffraction pattern (**b**) of a Pd NP after the reaction, showing that the particle remained a face-centered cubic Pd crystal, instead of forming carbide or oxide. Scale bar, 20 nm.

***In situ* HRTEM observation of the carbon gasification**

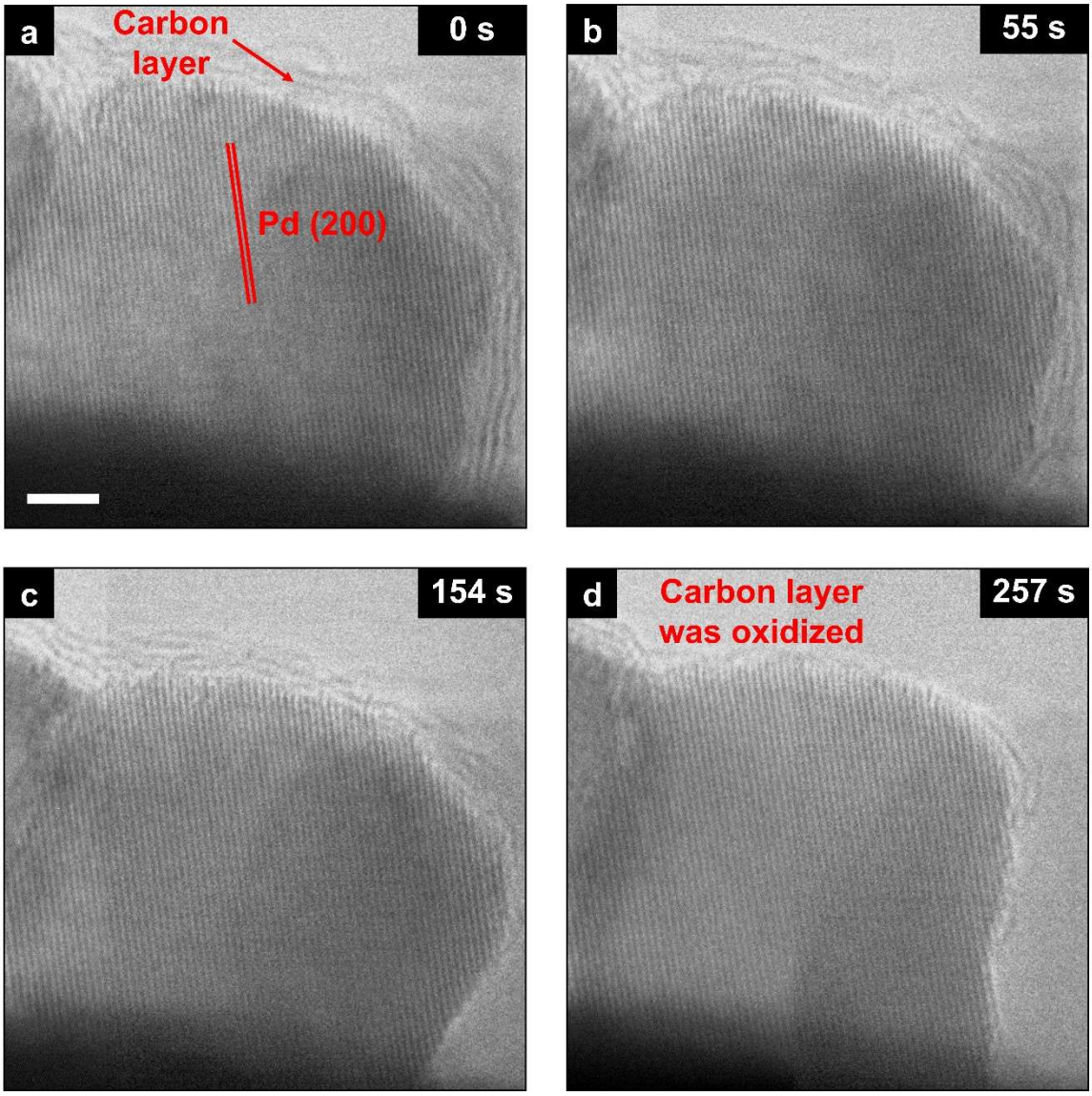

Supplementary Figure S4 | TEM snapshots from an *in situ* HRTEM movie. The Pd NP was immersed in 0.2 Pa oxygen atmosphere after being heated up to 300 °C. The lattice fringes correspond to the Pd (200) planes. The surface carbon layer was finally oxidized and removed. Scale bar, 2 nm.

Surface diffusion-dominated migration of a bi-grained particle

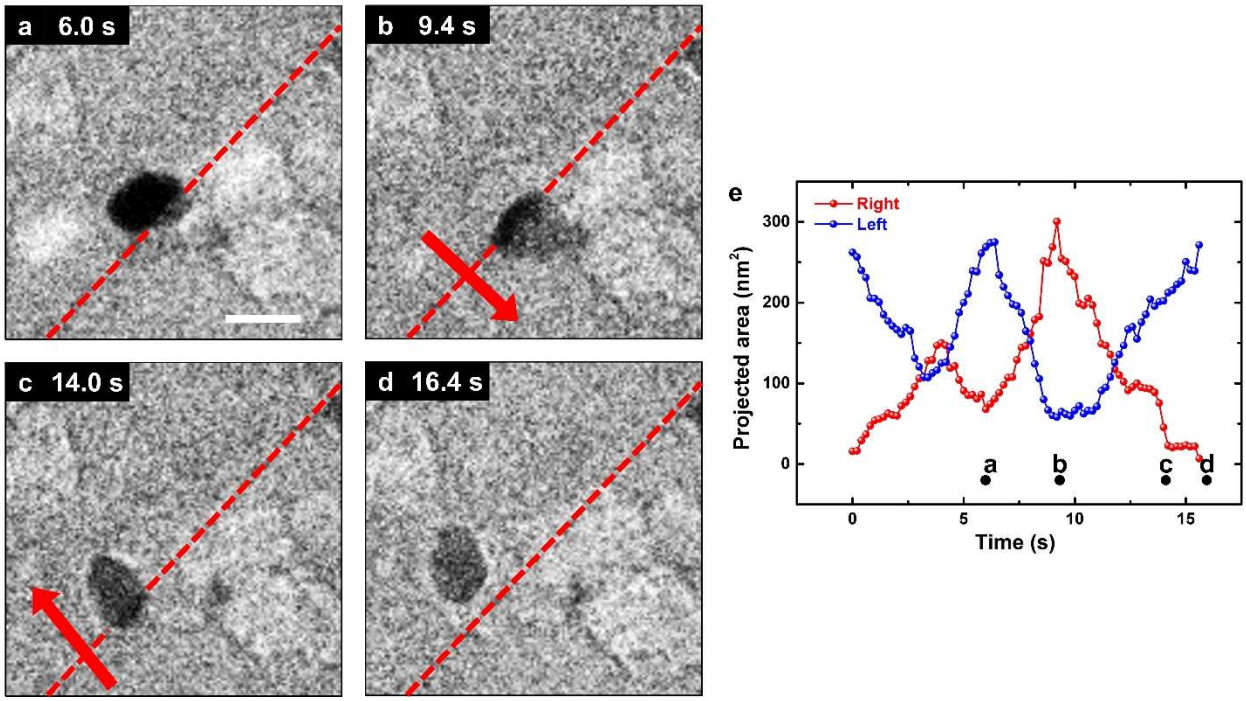

Supplementary Figure S5 | a-c, The bi-grained particle can only migrate along the red dashed line, i.e. its grain boundary, with its mass swung around it. **d**, Once all the mass was transported to one side, the bi-grained particle became a single-grained particle and was able to move away from the red dashed line. Scale bar, 20 nm. **e**, The projected area of both sides underwent an oscillatory evolution alternately. See Supplementary Movie S5.

Supplementary Movie S1

Self-propelled locomotion of 6 Pd NPs

under 0.2 Pa oxygen at 300 ºC (20X actual speed)

Supplementary Movie S2

Contagious mobilization of the initially-still particle by the mobile one

under 0.2 Pa oxygen at 300 ºC (4X actual speed)

Supplementary Movie S3

Elongation-contraction oscillatory shape transition and peristaltic migration of Pd NPs

under 0.2 Pa oxygen at 300 ºC (2X actual speed)

Supplementary Movie S4

Particle fission after fusion

under 0.2 Pa oxygen at 300 ºC (4X actual speed)

Supplementary Movie S5

Multi-grained particle swinging around its grain boundary which was kept along the red dashed line

under 0.2 Pa oxygen at 300 ºC (2X actual speed)

Supplementary Movie S6

Shadow images with bright contrast appearing occasionally during particle migration

under 0.2 Pa oxygen at 300 ºC (4X actual speed)

References

1 Lim, B. et al. New insights into the growth mechanism and surface structure of palladium nanocrystals. Nano Research 3, 180-188 (2010).

2 Zhang, H., Jin, M., Xiong, Y., Lim, B. & Xia, Y. Shape-controlled synthesis of Pd nanocrystals and their catalytic applications. Accounts of chemical research 46, 1783-1794 (2012).